Assessment of oil potentials for humic coals on the basis of flash Py-GC, Rock-Eval and confined pyrolysis experiments

Lifei Zeng [a,b], Wenkui Huang [a,b], Changchun Pan [a,*], Jun Jin [c], Wanyun Ma [c], Shuang Yu [a], Hao Xu [d,e], Dayong Liu [a], Yuhong Liao [a], Jinzhong Liu [a]

[a] *State Key Laboratory of Organic Geochemistry, Guangzhou Institute of Geochemistry, Chinese Academy of Sciences, Wushan, Guangzhou 510640, China*
[b] *University of Chinese Academy of Sciences, Beijing 100049, China*
[c] *Research Institute of Experiment and Testing, Xinjiang Oilfield Company, PetroChina, Karamay, Xinjiang 834000, China*
[d] *School of Environment and Energy, South China University of Technology, Guangzhou 510006, China*
[e] *Dongguan Environmental Monitoring Centre Station, Dongguan 523000, China*

ABSTRACT

Confined pyrolysis experiments (gold capsules), quantitative flash pyrolysis-gas chromatography (Py-GC) and Rock-Eval analysis were performed on ten coals from the Junggar Basin and seven coals from the Kuqa Depression, Tarim Basin, northwestern China. The maximum yields of liquid components in confined pyrolysis experimnets ($MCP\Sigma C_{8+}$), which reflect oil potentials, have close correlations with the yields of n-alkanes + n-alkenes ($FP\Sigma n$-C_{7+}) in flash Py-GC, but have poor correlations with Rock-Eval QI (($S1 + S2$)/TOC) values. Thus, oil potentials of coals can be better predicted on the basis of $FP\Sigma n$-C_{7+} yields from flash Py-GC analysis. Coals with $FP\Sigma n$-C_{7+} yield >10.4 mg/g TOC can generate $MCP\Sigma C_{8+}$ yield >∼22.5 mg/g TOC or oil yield >∼40 mg/g TOC in confined pyrolysis or in natural systems and are effective oil source rocks. Although both Py-GC and Rock-Eval are open systems, the yields of total liquid components ($FP\Sigma C_{7+}$) obtained from flash Py-GC have poor correlations with, and are substantially lower than, Rock-Eval QI. In contrast, $FP\Sigma C_{7+}$ values have much better correlations with oil potentials ($MCP\Sigma C_{8+}$). Coals with higher oil potentials ($MCP\Sigma C_{8+}$) generate higher amounts of liquid components detected in flash Py-GC ($FP\Sigma C_{7+}$) than those with lower oil potentials but similar Rock-Eval QI. The correlations for parameters with gas to oil ratios (GOR) in confined pyrolysis are increasingly better in the sequence of Rock-Eval QI, H/C atomic ratios, $MCP\Sigma C_{8+}$, $FP\Sigma n$-C_{7+} and $FP\Sigma n$-$C_{7+}/\Sigma C_{7+}$ ratios. GOR of petroleum generated from coals within oil generative window can be reasonably predicted on the basis of $FP\Sigma n$-$C_{7+}/\Sigma C_{7+}$ ratio from flash Py-GC analysis.

© 2020 Elsevier Ltd. All rights reserved.

1. Introduction

Coal is mainly a source of gas, but it can be also a source of oil under some circumstances (e.g., Hunt, 1991). Humic coals and terrigenous organic matter are highly heterogeneous in chemical composition. The releasable components from kerogen of humic coals are mainly aromatic compounds and phenols (Peters, 1986; Katz et al., 1991; Tegelaar and Noble, 1994; Isaksen et al., 1998). Methods to evaluate the oil potential of humic coals can be different from those for oil-prone source rocks (e.g., Peters, 1986; Isaksen et al., 1998; Sykes and Snowdon, 2002). Rock-Eval hydrogen index (HI), H/C atomic ratio and maceral composition are widely used and excellent parameters to evaluate oil potential

for oil-prone source rocks (e.g., Tissot and Welte, 1984; Peters et al., 2005), but are frequently not effective indicators of oil potential for coals and terrigenous organic matter (e.g., Powell and Boreham, 1991; Curry et al., 1994, 1995; Curry, 1995; Isaksen et al., 1998; Killops et al., 1998). Previous studies have suggested that the concentration of C_{8+} aliphatic groups (n-alkanes + n-alkenes) determined by pyrolysis–gas chromatography (Py-GC) could be a better indicator of oil generative potential for coals and terrigenous organic matter (Curry et al., 1995; Curry, 1995; Isaksen et al., 1998). Isaksen et al. (1998) demonstrated that humic coals from the Middle Jurassic Sleipner Formation in the North Sea with HI in the range of 220–415 mg HC/g TOC have lower concentrations of C_{15+} aliphatic groups (n-alkanes + n-alkenes) in the range of 64–553 counts/µg TOC while a coal from the Eocene strata of the Taranaki Basin, New Zealand with HI 362 mg HC/g TOC has a substantially higher concentration of C_{15+} aliphatic groups of 4001 counts/µg TOC determined by sem-quantitative Py-GC analysis.

* Corresponding author.
  E-mail address: cpan@gig.ac.cn (C. Pan).

The former are primarily gas-prone but the latter is capable of generating non-volatile oil on the basis of exploration results (Isaksen et al., 1998).

The precise amounts of oil and hydrocarbon gases generated from a source rock can only be obtained by pyrolysis experiments under conditions that are comparable to the natural environment (e.g., Price and Wenger, 1992). Previous studies have demonstrated that the pyrolysates from confined pyrolysis using gold capsules on kerogens and coals are very similar to oils in reservoirs and bitumen extracted from source rocks (Monthioux et al., 1985, 1986; Mansuy and Landais, 1995; Mansuy et al., 1995; Michels et al., 2000; Li et al., 2013; Xiang et al., 2016). Oil yields determined from confined pyrolysis could reflect those generated from source rocks by geological processes.

In the Kuqa Depression of the northern Tarim Basin, northwestern China (Fig. 1b), a huge amount of gas has been found with total in-place reserves over 1×10^{12} m³, which was derived from coaly source rocks within the Triassic-Jurassic strata (e.g., Liang et al., 2003; Zhao et al., 2005; Wang, 2014). In addition, a minor amount of oil has been also found which was derived from these coaly source rocks in the depression (e.g., Liang et al., 2003; Zhao et al., 2005). In the Junggar Basin, northwestern China, two gas fields (Mahe and Hutubi gas fields) and seven oilfields (Cainan, Qigu,

Duoshanzi, Gaoquan, Kayindike, Chunfeng and Chunguang oilfields) have been found (Fig. 1a), in which oil and gas components were mainly derived from Jurassic coaly source rocks (Chen et al., 2003a,b, 2015; Wang et al., 2013; Xiao et al., 2014; Sun et al., 2015; Du et al., 2019). In particular, oil tests have demonstrated an oil production rate of 1213 m³ and a gas production rate of 322×10^3 m³ per day from the interval around 5770 m within the Cretaceous strata in a newly drilled borehole GT1 in the Gaoquan oilfield in the Sikeshu sag, southwestern Junggar Basin (Fig. 1a), the highest oil production rate for all boreholes drilled over 70 years in the basin (Du et al., 2019). This discovery stimulated a new round of extensive petroleum exploration in this region.

Flash pyrolysis-gas chromatography (Py-GC) has been used to obtain information on chemical structure and composition of releasable moieties of kerogen (e.g., Larter and Douglas, 1980; Largeau, 1984; Eglinton et al., 1988, 1991; Horsfield, 1989; Derenne et al., 1990; Tegelaar and Noble, 1994). The primary aim of the present study was to establish the correlations between parameters, i.e. the amount of liquid aliphatic components (C_{7+} *n*-alkanes + *n*-alkenes) obtained by quantitative flash Py-GC, and the oil yield determined from confined pyrolysis experiments on humic coals from the Junggar Basin and Kuqa Depression of the
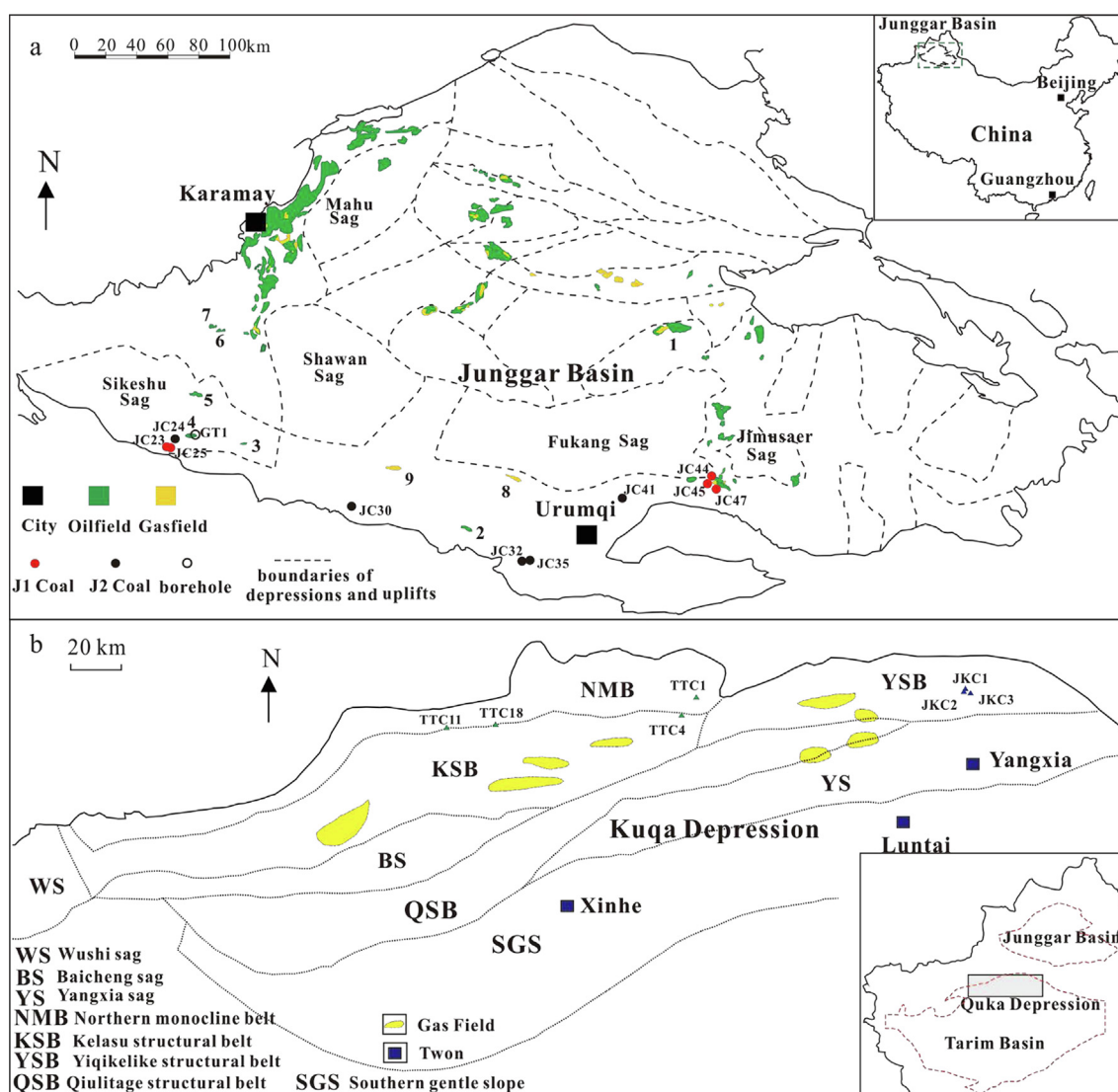

Fig. 1. Location map of the Junggar Basin and Kuqa Depression and sample locations. In figure (a), 1: Cainan oilfield; 2: Qigu oilfield; 3: Dushanzi oilfield; 4: Gaoquan oilfield; 5: Kayindike oilfield; 6: Chunguang oilfield; 7; Chunfeng oilfield; 8: Hutubi gas field; 9: Mahe gas field.

Tarim Basin. Oil yield varies substantially from one coal sample to another even within the same coal bed in a region due to compositional heterogeneity. Confined pyrolysis is not a routine approach and it is costly to obtain the oil yield of a coal by a series of confined pyrolysis experiments. In contrast, flash Py-GC and Rock-Eval analyses are conveniently available and readily applied analytical techniques. It is useful to establish a correlation between oil yields from confined pyrolysis and parameters from flash Py-GC and Rock-Eval analyses for coals and to predict oil yields of coals under geological condition on the basis of parameters from flash Py-GC and Rock-Eval analyses.

2. Samples and experimental

2.1. Samples

Coal beds are mainly found within the Lower Jurassic Badaowan Formation (J_1b) and Middle Jurassic Xishanyao Formation (J_2x) in the Junggar Basin. In the present study, ten coals from this basin were used for confined pyrolysis experiments and flash Py-GC analysis. Among these ten coals, five were collected within the Lower Jurassic Badaowan Formation (J_1b) while the other five were collected within the Middle Jurassic Xishanyao Formation (J_2x, Table 1, Fig. 1a).

Coal beds in the Kuqa Depression of the Tarim Basin are within the Upper Triassic Taliqike Formation (T_3t), the Lower Jurassic Yangxia Formation (J_1y) and the Middle Jurassic Kezilenuer Formation (J_2k). In a previous study, we performed confined pyrolysis experiments on four coals from the Upper Triassic Taliqike Formation (T_3t, TTC1, TTC4, TTC11 and TTC18) and three coals from the Middle Jurassic Kezilenuer Formation (J_2k, JK1, JK2 and JK3) to determine oil and gas yields and kinetic parameters for oil and gas generation (Table 1, Fig. 1b; Huang et al., 2019). In the present study, we performed flash Py-GC analysis on these coals to document geochemical controls on oil yields in confined pyrolysis.

All coal samples from both the Junggar Basin and Kuqa Depression of Tarim Basin were collected from coal pits (Fig. 1). As introduced previously (Huang et al., 2019), these coals were first cleaned and then ground into powder (about 200 mesh). A small aliquot of powder (about 40 mg) was taken from each sample for

measurement of total organic carbon content (TOC) using a Leco-230 C/S analyzer. Another small aliquot of powder (about 10 mg) was taken for Rock-Eval analysis using an IFP Rock-Eval 6. For each coal, about 2 g of powder was treated with HCl and HF to obtain kerogen and about 3 mg of kerogen was used for organic elemental analysis (CHN) using an Elementar Vario EL III.

For the measurement of vitrinite reflectance (%Ro), polished sections were prepared on coal lumps. Vitrinite reflectance was measured on the polished sections using a Leica DMRX microscope equipped with a 3Y PostPro V.2.0.0 microphotometer. Three standards – sapphire, yttrium-aluminum-garnet and cubic zirconia with reflectance (%Ro) 0.596, 0.904 and 3.11, respectively – were used to calibrate the measurements. An oil immersion objective 50/0.85 lens was used with measured dimension about 7 μm in diameter. Mean random vitrinite reflectance (%Ro) is reported from the average value of about 50 measurements.

2.2. Confined pyrolysis experiments

The method for confined pyrolysis experiments on the coals is similar to that described in our previous studies (Li et al., 2013; Xiang et al., 2016; Huang et al., 2019). Briefly, gold capsules were loaded a weighed amount of coal powder without extraction (30–50 mg) and placed in steel pressure vessels. The internal pressure of the vessels, connected to each other with tubing, was maintained at 50 MPa with an error < ± 0.1 MPa, by pumping water into or out of the vessels during the experiments. The vessels were heated in a furnace from room temperature to 250 °C over 10 h, and then, from 250 °C to 431 °C at a rate of 2 °C/h. Two thermocouples were used to measure the temperature of the pyrolysis experiments and to check each other. The error of the recorded temperatures is < ± 1 °C. Vessels containing gold capsules were removed from the oven at temperature intervals of 12 °C or 24 °C between from ~322 to ~431 °C.

2.3. Analysis of gas components

After pyrolysis, the volatile components in the capsules were collected in a special sampling device connected to a modified Agilent 6890 GC, as described previously (Li et al., 2013; Xiang et al.,

Table 1
Geochemical parameters from Rock-Eval, confined pyrolysis and flash Py-GC for coals.

	Strata	TOC (%)	%Ro	S1	S2	QI	Tmax	MCP Σn-C8+	MCP ΣC8+	MCP ΣC8+/QI	CPΣ C1-5	CPΣC1-5/ΣC8+	FPΣn-C7+	FPΣ C7+	FPΣn-C7+/ΣC7+	C (%)	H (%)	N (%)	H/C
Coals from the Junggar Basin																			
JC23	J_1b	62.39	0.39	0.7	107	173	428	36.2	71.1	0.41	32.1	0.45	37.0	124	0.30	73.59	5.36	0.84	0.87
JC25	J_1b	62.21	0.42	0.7	96	156	424	31.8	69.1	0.44	35.3	0.51	27.6	96	0.29	72.35	5.15	0.72	0.85
JC44	J_1b	73.23	0.76	4.0	141	197	440	15.1	55.9	0.28	34.7	0.62	23.5	117	0.20	81.47	4.83	0.96	0.71
JC45	J_1b	70.81	0.74	7.8	136	203	448	11.9	49.5	0.24	36.2	0.73	19.9	115	0.17	84.26	5.04	0.75	0.72
JC47	J_1b	80.28	0.72	7.4	150	196	453	17.1	60.1	0.31	28.6	0.48	25.4	126	0.20	85.20	5.14	0.84	0.72
JC24	J_2x	58.63	0.52	2.1	152	262	422	55.0	120.4	0.46	53.4	0.44	48.8	159	0.31	71.73	6.10	0.72	1.02
JC30	J_2x	73.33	0.58	1.6	103	143	432	27.5	44.9	0.31	15.9	0.35	38.7	101	0.38	80.57	5.28	0.66	0.79
JC32	J_2x	65.89	0.50	1.2	134	205	424	22.3	45.9	0.22	29.3	0.64	28.1	111	0.25	73.33	5.60	0.79	0.92
JC35	J_2x	63.60	0.50	0.9	134	212	425	26.1	59.4	0.28	33.7	0.57	39.5	114	0.34	72.64	5.81	0.53	0.96
JC41	J_2x	69.61	0.67	1.8	108	158	439	17.4	37.5	0.24	15.6	0.42	25.3	97	0.26	82.00	5.23	0.62	0.77
Coals from the Kuqa Depression																			
JKC1	J_2k	71.91	0.58	2.9	101	145	424	4.5	19.9	0.14	11.8	0.60	10.1	72	0.14	75.44	4.42	0.40	0.70
JKC2	J_2k	74.42	0.66	4.5	136	189	437	5.7	22.4	0.12	14.0	0.63	10.0	81	0.12	82.19	4.77	0.94	0.70
JKC3	J_2k	72.84	0.62	0.3	42	58	433	2.1	8.1	0.14	7.7	0.95	2.5	32	0.08				
TTC1	T_3t	75.28	0.73	4.2	208	282	433	15.2	46.9	0.17	18.2	0.39	33.9	108	0.31	81.06	5.23	1.11	0.77
TTC4	T_3t	77.25	0.74	4.8	172	229	447	5.5	24.8	0.11	25.2	1.01	12.3	107	0.11	85.39	4.98	1.08	0.70
TTC11	T_3t	70.54	0.58	4.2	196	284	437	10.9	38.2	0.13	17.3	0.45	24.0	108	0.22	83.41	5.10	0.84	0.73
TTC18	T_3t	79.27	0.74	9.6	200	265	458	9.2	35.2	0.13	16.8	0.48	14.9	68	0.22	88.08	6.36	1.18	0.87

TOC, Rock-Eval, confined pyrolysis and flash Py-GC were performed on coal powders without extraction. C(%), H(%) and N(%) were measured on kerogen samples. Rock-Eval parameters S1 and S2: in "mg HC/g coal"; QI=(S1 + S2)/TOC: in "mg HC/g TOC"; Tmax: in "°C"; Parameters from confined pyrolysis, MCPΣn-C8+ (maximum yield of n-alkanes), MCPΣC8+ (maximum yield of total liquid components) and CPΣC1-5 (gas yield at the maturity for MCPΣC8+): in "mg/g TOC"; CPΣC1-5/ΣC8+: in "mg/mg"; Parameters from flash PY-GC, FPΣn-C7+ and FPΣC7+: in mg/g TOC; TOC, Rock-Eval and confined pyrolysis data for coals from the Kuqa Depression from Huang et al. (2019). For coal JK3, MCPΣC8+ was calculated on the basis of MCPΣn-C8+ (Huang et al., 2019).

2016; Huang et al., 2019). Briefly, the device was first evacuated to <1 × 10⁻² Pa at room temperature (25 °C). The gold capsule was then pierced with a needle under vacuum, allowing the gases to escape into the device. The valve connecting the device and the modified GC was open to allow the gas to enter the GC, through which the GC analyses of both the organic and inorganic gas components were performed in an automatically controlled procedure. The oven temperature for the hydrocarbon gas analysis was initially held at 70 °C for 6 min, ramped from 70 °C to 130 °C at 15 °C/min, from 130 °C to 180 °C at 25 °C/min, and then held at
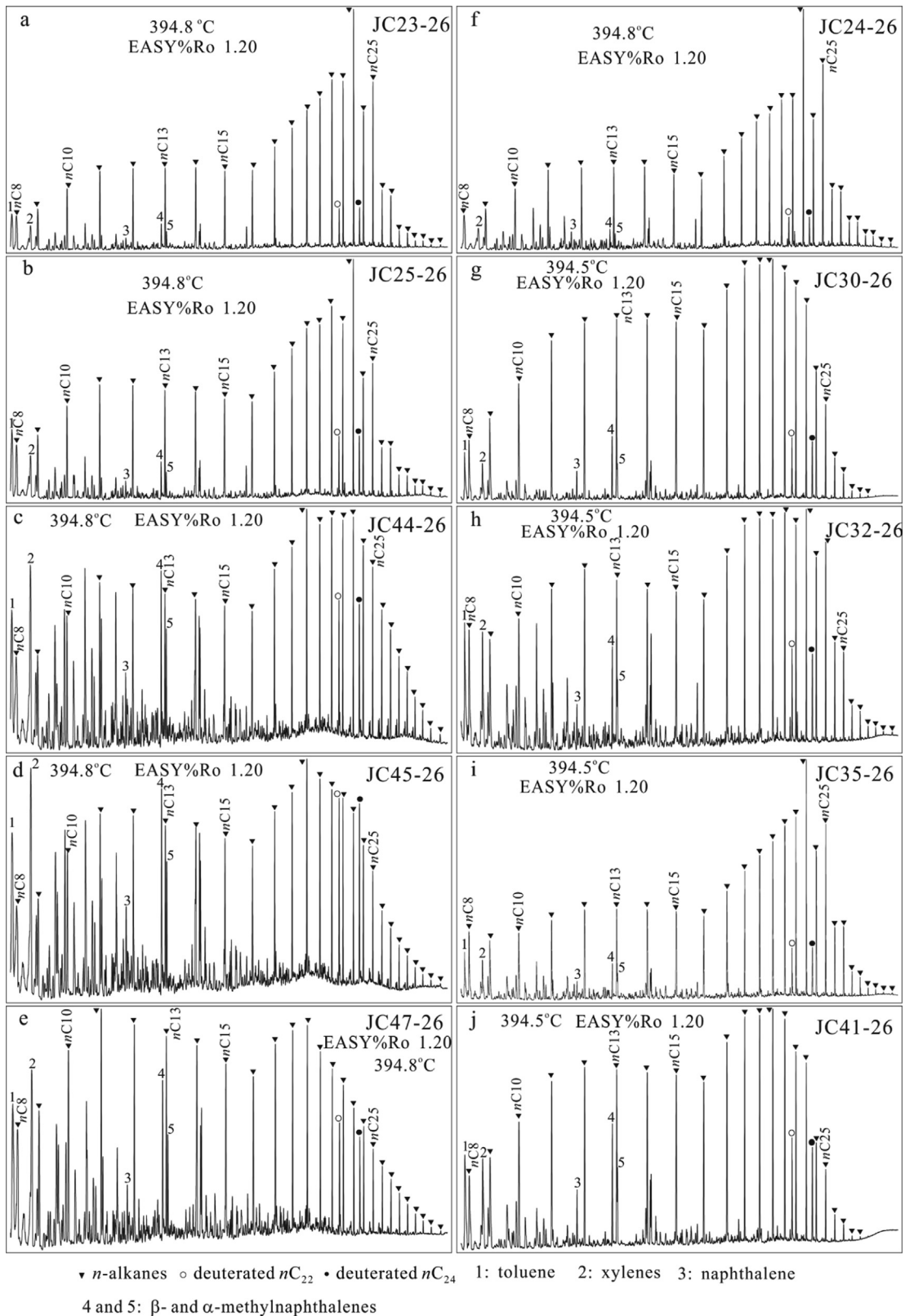
Fig. 2. Gas chromatograms of liquid hydrocarbons at about 395 °C for ten coals from the Junggar Basin at a heating rate 2 °C/h in confined pyrolysis experiments.

180 °C for 4 min, whereas it was held at 90 °C for the inorganic gas analysis. The analysis of all gases was carried out by one single injection. A test with external standard gases (CH$_4$:C$_2$H$_6$:C$_3$H$_8$: CO$_2$:N$_2$ = 5:3:2:5:85 by volume) indicated that the amounts of gas products measured using this device had better than 0.5% relative error.

2.4. Analyses for liquid components (ΣC_{8+})

The method for the analysis of liquid components (ΣC_{8+}) is similar to that described in previous studies (Li et al., 2013; Xiang et al., 2016; Huang et al., 2019). After analysis for gas components, the capsules were cut swiftly into pieces in a vial, which contained
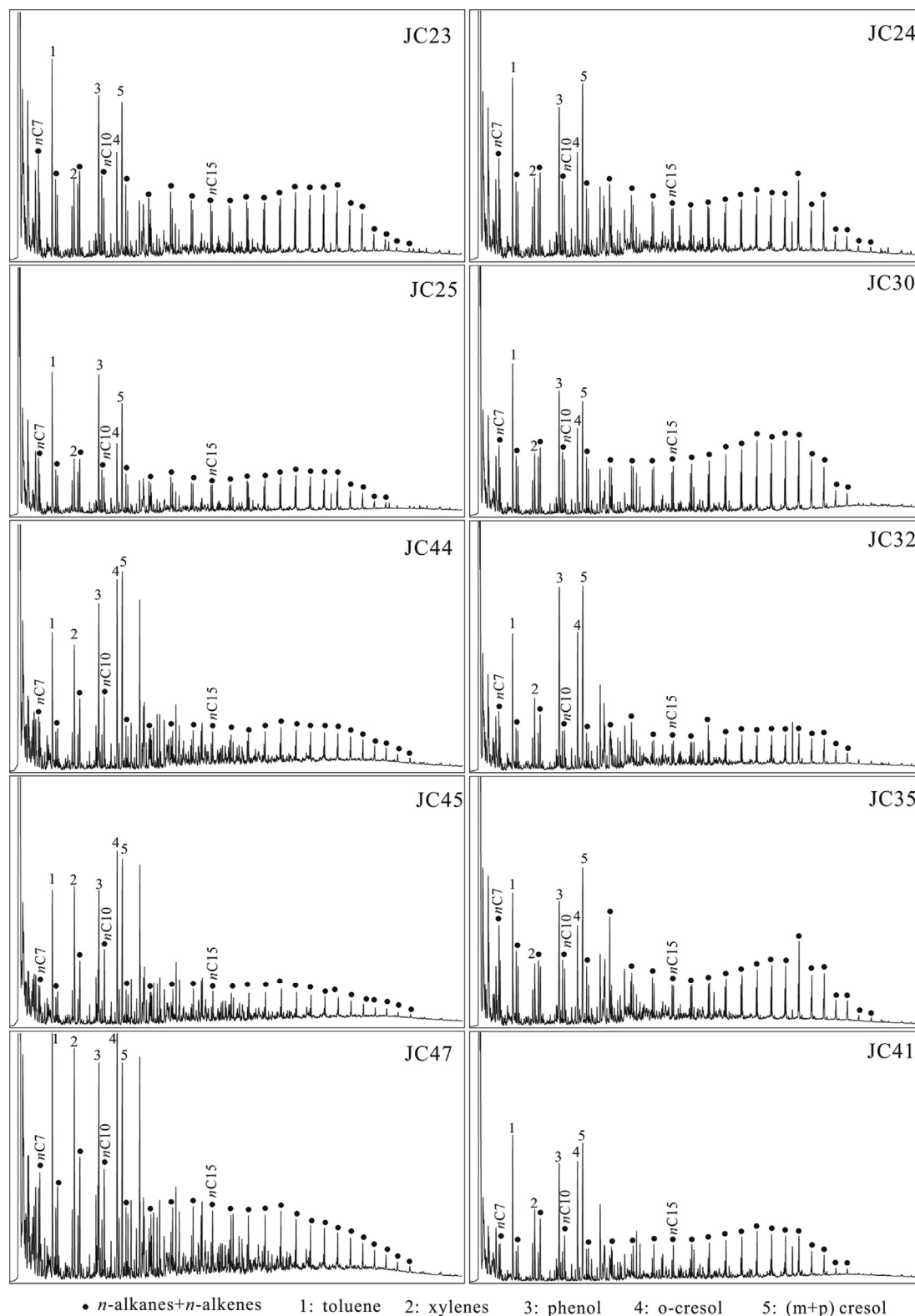
Fig. 3. Flash Py-gas chromatograms for ten coals from the Junggar Basin.

• n-alkanes+n-alkenes   1: toluene   2: xylenes   3: phenol   4: o-cresol   5: (m+p) cresol

about 3 ml pentane. Two internal standards of deuterated n-C_{22} and n-C_{24} were then added to each vial both with amounts ranging from 0.010 mg to 0.015 mg. Following five ultrasonic treatments of 5 min per treatment, these vials were allowed to settle for 72 h until the pentane solutions became clear. The pentane solutions in all vials were directly injected into a HP6890 GC fitted with a 30 m × 0.32 mm i.d. column coated with a 0.25 μm film of HP-5, employing nitrogen as carrier gas. The oven temperature was programmed as follows: 50 °C for 5 min, raised from 50 °C to 150 °C at 2 °C/min, and from 150 °C to 290 °C at 4 °C/min, and then held at 290 °C for 15 min.

2.5. Flash Py-GC analysis

Flash Py-GC analysis on coal samples was performed on a CDS-5150 pyroprobe connected to a Thermo Scientific Trace GC Ultra gas chromatograph, similar to that introduced previously (Liao et al., 2015; Pan et al., 2015). Coal powders (1–2 mg) without extraction were weighed and loaded into a quartz tube. The quartz tube was then placed into the pyrolysis apparatus. The platinum wire loop of the probe was heated to 100 °C for 1 min in a helium flow to dry the coal powder, then ramped to 650 °C at a rate of 5000 °C/s and held isothermally for 20 s. A 30 m × 0.25 mm i.d. DB-1 column (film thickness 0.25 μm) was used. The injector was kept at 300 °C. The GC oven temperature was initially held at 40 °C for 2 min, raised from 40 to 305 °C at a rate of 4 °C/min, and then held at 305 °C for 20 min. Nitrogen was used as a carrier gas at a constant flow rate of 1.5 ml/min.

Pyrolysis products were quantified using an external standard of polymethylstyrene. Four quartz tubes with quartz wool at one end were added with 2.09, 4.18, 6.27 and 8.35 μg of polymethylstyrene, respectively. The pyrolysis and GC analysis conditions of the standard were identical to that of the coal powder. A response factor was obtained from the external standard runs. The amount of pyrolysis products from coal powder was quantified using this response factor.
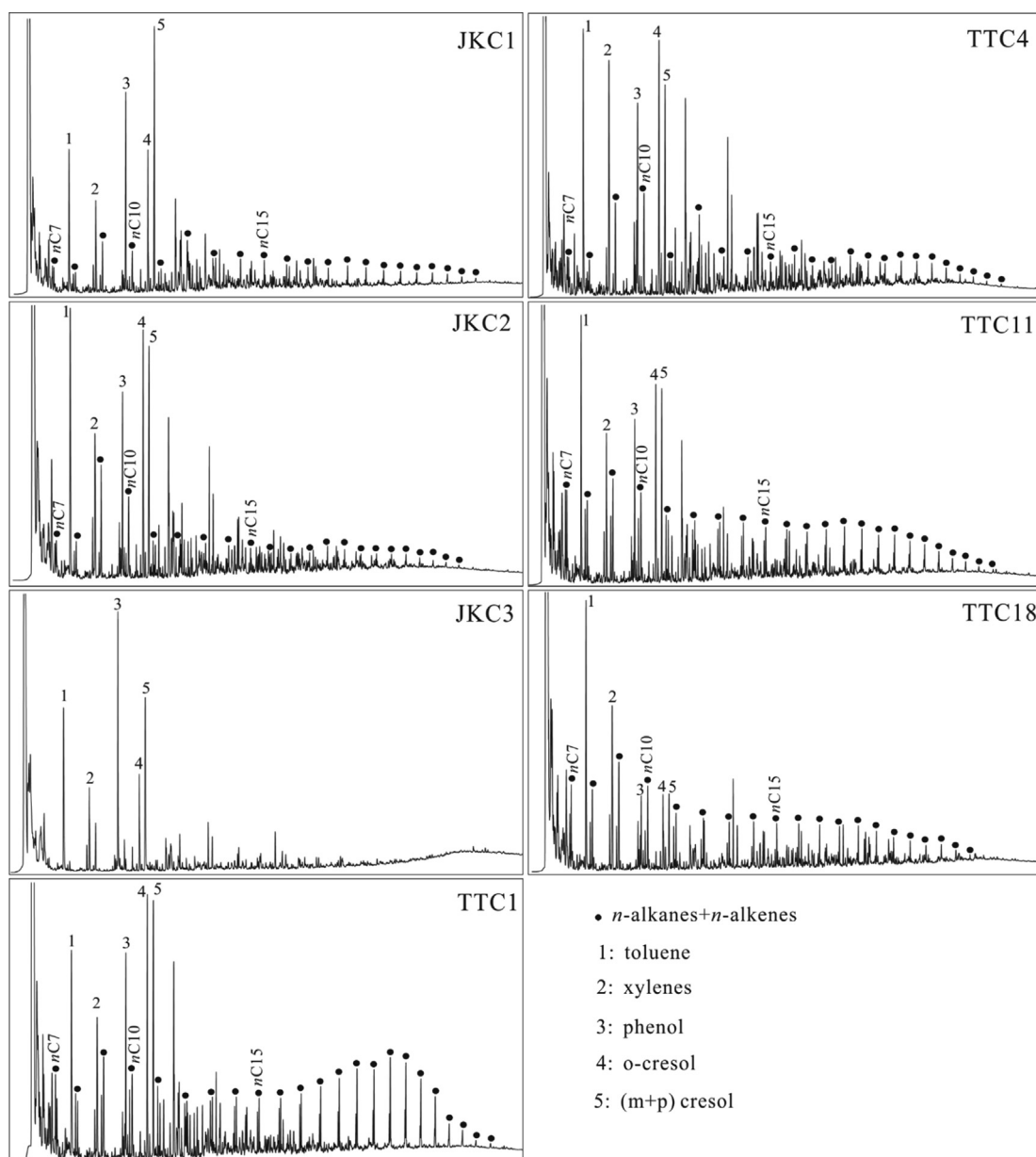

Fig. 4. Flash Py-gas chromatograms for seven coals from the Kuqa Depression, Tarim Basin.

3. Results

Rock-Eval parameters and the yields of liquid and gas components determined from confined pyrolysis experiments and quantitative flash Py-GC are demonstrated in Table 1. Gas chromatograms of liquid components in confined pyrolysis at 395 °C at 2 °C/h on ten coals from the Junggar Basin are demonstrated in Fig. 2. Gas chromatograms from flash Py-GC on ten coals from the Junggar Basin and seven coals from the Kuqa Depression of Tarim Basin are demonstrated in Figs. 3 and 4, respectively.

4. Discussions

4.1. Crossplot of yields of liquid components (ΣC_{8+}) from confined pyrolysis vs Rock-Eval QI values

In confined pyrolysis, for the ten coals from the Junggar Basin, liquid components are dominated by n-alkanes, similar to the non-biodegraded oils in natural reservoirs (Fig. 2). For the seven coals from Kuqa Depression, coal JKC3 produced a higher amount of aromatic components, strikingly different from non-
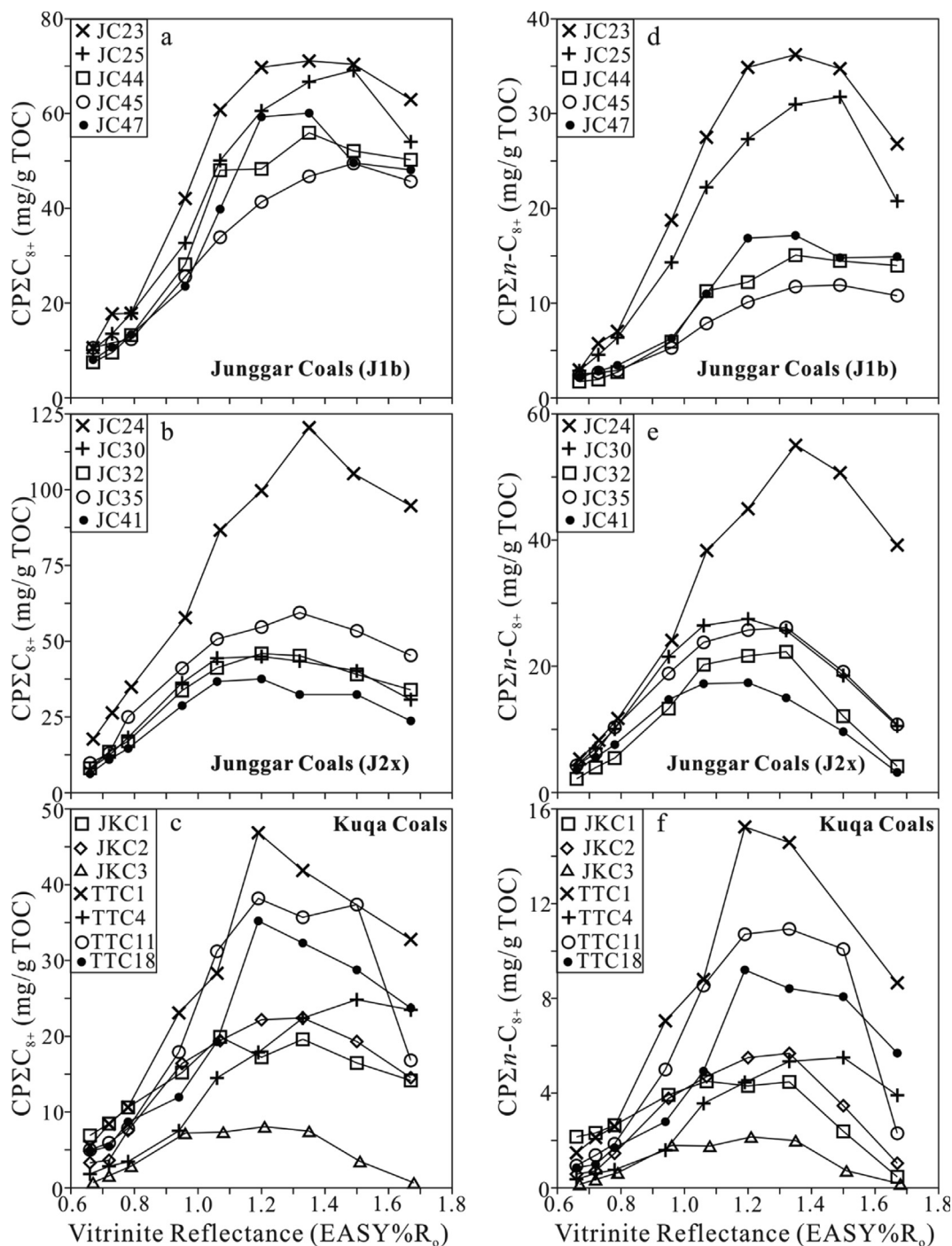

Fig. 5. Yields of total liquid components (CPΣC$_{8+}$) and n-alkanes (CPΣn-C$_{8+}$) in confined pyrolysis for the 17 coals from 322 °C to 431 °C at a heating rate 2 °C/h (EASY%Ro 0.66–1.67) in confined pyrolysis experiments (data for the seven coals from Kuqa Depression from Huang et al., 2019).

biodegraded crude oils while the other six coals produced mainly n-alkanes, similar to the non-biodegraded crude oils, as reported previously (Huang et al., 2019). In this paper, the yield of liquid components (ΣC_{8+}) in confined pyrolysis is defined as $CP\Sigma C_{8+}$. $CP\Sigma C_{8+}$ yields increase first to maximum values, and then decrease with EASY%Ro (Fig. 5a–c). Sweeney and Burnham (1990) presented a vitrinite maturation model to predict the vitrinite reflectance (% Ro) under geological condition, called EASY%Ro, using an Arrhenius first-order parallel-reaction approach with a distribution of activation energies. Later, EASY%Ro values were also used to estimate maturity in confined pyrolysis experiments (e.g., Hill et al., 2003; Li et al., 2013; Xiang et al., 2016; Huang et al., 2019). In this paper, EASY%Ro was used to indicate the maturity achieved at various temperatures. The maximum $CP\Sigma C_{8+}$ values, defined as $MCP\Sigma C_{8+}$ for the 17 coals are shown in Table 1. We assume that $MCP\Sigma C_{8+}$ values reflect the oil potentials (oil yields) of these coals under geological conditions as documented in previous studies (Monthioux et al., 1985, 1986; Mansuy et al., 1995; Mansuy and Landais, 1995; Michels et al., 1995; Li et al., 2013; Xiang et al., 2016; Huang et al., 2019).

Rock-Eval parameter QI, defined as (S1 + S2)/TOC by Pepper and Corvi (1995), is widely used to evaluate the petroleum generative potentials of source rocks. The correlation between $MCP\Sigma C_{8+}$ and QI is very poor for the 17 coals (Fig. 6a). Previous study has demonstrated that only a portion (38–53%) of the releasable moieties in

Rock-Eval analysis contribute to the formation of oil and gaseous hydrocarbons in confined pyrolysis at EASY%Ro 1.19–1.50% for the seven coals from Kuqa Depression (Huang et al., 2019). The results of the present study demonstrate that the ratios of $MCP\Sigma C_{8+}/QI$ vary over a wide range for the 17 coals, i.e. 0.22–0.46 for the ten coals from the Junggar Basin and 0.11–0.17 for the seven coals from the Kuqa Depression (Table 1). This ratio reflects the portion of releasable components in Rock-Eval analysis contributing to oil generation in confined pyrolysis or under geological condition, and indicates that coals from the Junggar Basin generate higher amounts of oil compared with those from the Kuqa Depression with similar QI values (Table 1, Fig. 6a).

4.2. Yield crossplot of n-alkanes (Σn-C_{8+}) in confined pyrolysis vs aliphatic components (ΣC_{7+} n-alkanes + n-alkenes) in flash Py-GC

Here, we define the yields of n-alkanes (Σn-C_{8+}) in confined pyrolysis as $CP\Sigma n$-C_{8+}, and the yields of aliphatic components (ΣC_{7+} n-alkanes + n-alkenes) in flash Py-GC as $FP\Sigma n$-C_{7+}. $CP\Sigma n$-C_{8+} increases first to maximum values, and then decreases with EASY%Ro (Fig. 5d–f), similar to $CP\Sigma C_{8+}$ (Fig. 5a–c). The maximum $CP\Sigma n$-C_{8+} ($MCP\Sigma n$-C_{8+}) and $FP\Sigma n$-C_{7+} values for the 17 coals are shown in Table 1.

In flash Py-GC analysis, all the 17 coals released components with high amounts of aromatic compounds (e.g., toluene and xyle-
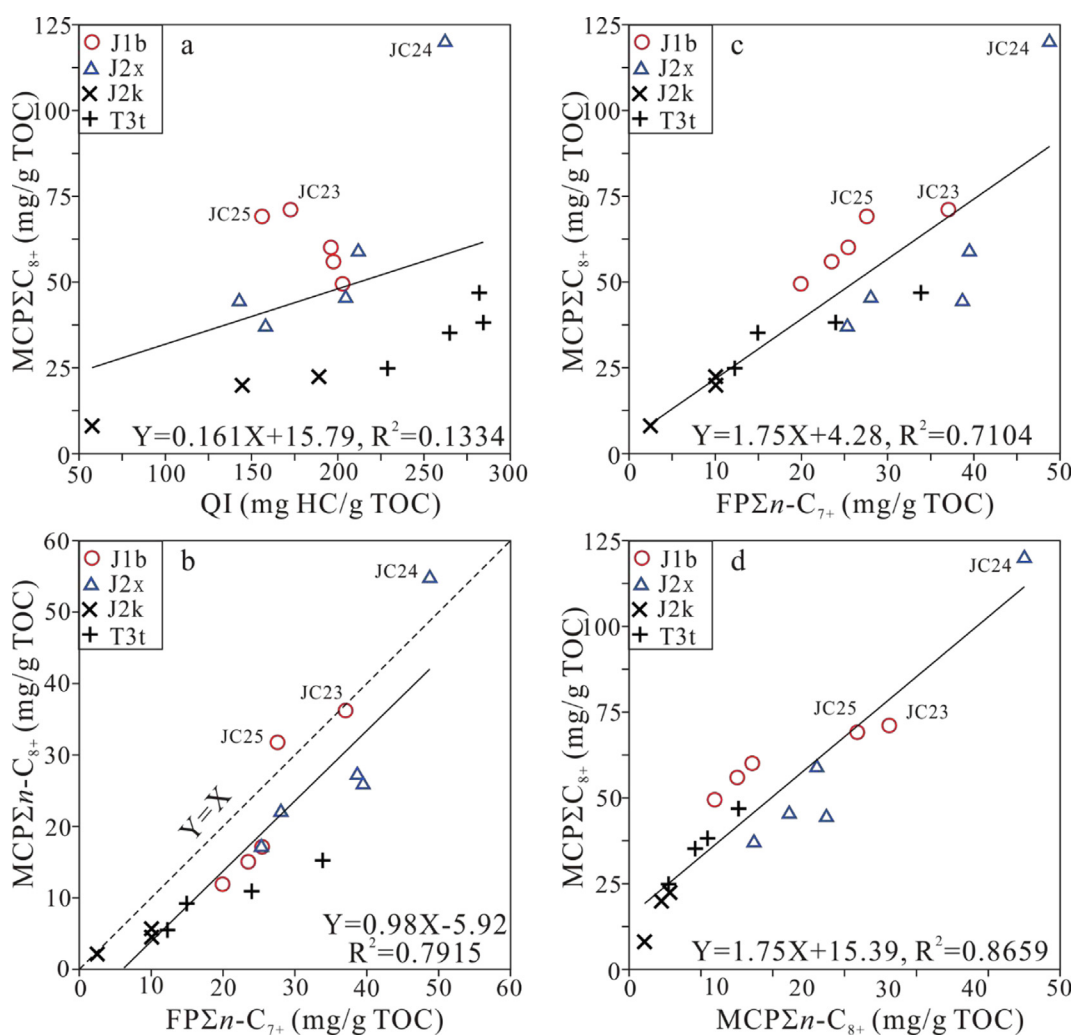

Fig. 6. Crossplots of parameters form confined pyrolysis, Rock-Eval and flash Py-GC. (a) Rock-Eval QI vs the maximum $CP\Sigma C_{8+}$ from confined pyrolysis; (b) $FP\Sigma n$-C_{7+} from flash Py-GC vs maximum $CP\Sigma n$-C_{8+} from confined pyrolysis; (c) $FP\Sigma n$-C_{7+} from flash Py-GC vs maximum $CP\Sigma C_{8+}$ from confined pyrolysis; (d) maximum $CP\Sigma n$-C_{8+} vs maximum $CP\Sigma C_{8+}$ from confined pyrolysis.

nes) and phenols (Figs. 3 and 4), in contrast to pyrolysates in confined pyrolysis (Fig. 2). However, FPΣn-C$_{7+}$ values have a good correlation with MCPΣn-C$_{8+}$ for the 17 coals (Fig. 6b): MCPΣn-C$_{8+}$ = 0.98 × FPΣn-C$_{7+}$ – 5.92 with R^2 = 0.79.

There are several causes influencing the correlation between FPΣn-C$_{7+}$ and MCPΣn-C$_{8+}$: (1) CPΣn-C$_{8+}$ and FPΣn-C$_{7+}$ were quantified using different approaches. CPΣn-C$_{8+}$ from confined pyrolysis was quantified using internal standards of deuterated n-C$_{22}$ and n-C$_{24}$ alkanes while FPΣn-C$_{7+}$ from flash Py-GC was quantified using an external standard of polymethylstyrene; (2) Only a portion, or even a minor portion of the bound n-alkane moieties can be released in both confined pyrolysis and flash Py-GC analysis from coal kerogen. In confined pyrolysis of a closed system, oil components are released from kerogen on the one hand and incorporated into kerogen on the other (e.g., McNeil and BeMent, 1996; Boreham et al., 1999; Dieckmann et al., 2006; Erdmann and Horsfield, 2006; Pan et al., 2012; Li et al., 2013, 2016; Burnham and Braun, 2017). In addition, the released oil components can be further decomposed to gases at EASY%Ro > 1.0. At this maturity for MCPΣn-C$_{8+}$, the n-alkane generation rate equals the rate of n-alkane decomposition to gases and reincorporation into kerogen. At this maturity level, a major portion of the initially bound n-alkanes remains attaching to aromatic rings in residual kerogen for gas-prone coals with low oil generative potentials (Li et al., 2013; Huang et al., 2019). In flash Py-GC analysis, coals were heated isothermally at 650 °C for only 20 s, and therefore, the bound components were certainly not released completely; (3) In flash Py-GC analysis, the released n-alkanes and n-alkenes may be partly generated from the degradation of bound isoalkanes, cyclic alkanes and even long chain alkyl aromatics due to high temperature. In addition, although the reincorporation of the released components to kerogen cannot be completely excluded, it occurs in much minor extent in flash Py-GC analysis compared with confined pyrolysis. Both causes possibly explain why FPΣn-C$_{7+}$ values are higher than MCPΣn-C$_{8+}$ for fifteen coals except coals JC24 and JC25 (Table 1, Fig. 6b).

FPΣn-C$_{7+}$ from flash Py-GC analysis have good correlations with MCPΣC$_{8+}$ from confined pyrolysis for the 17 coals with R^2 = 0.71 (Table 1, Fig. 6c), in contrast to Rock-Eval QI (Fig. 6a). This result supports the notion of previous studies that Rock-Eval HI is frequently not effective an indicator while the concentration of n-alkanes plus n-alkenes determined by Py-GC is a better indicator of oil generative potential for coals and terrigenous organic matter (e.g., Powell and Boreham, 1991; Curry et al., 1994, 1995; Curry, 1995; Isaksen et al., 1998).

The correlation between MCPΣn-C$_{8+}$ and MCPΣC$_{8+}$ is demonstrated in Fig. 6d. This correlation has R^2 = 0.87, reflecting the differences of n-alkane concentrations in oils generated from these 17 coals in confined pyrolysis. For ten coals from the Junggar Basin, six coals JC23, JC25, JC24, JC30, JC35 and JC41 generated higher amount of n-alkanes relative to other liquid components (Fig. 2a, b, f, g, i and j), compared with the other four coals JC44, JC45, JC47 and JC32 (Fig. 2c, d, e and h).

4.3. Differences in pyrolysate yields among Rock-Eval, flash Py-GC and confined pyrolysis

We defined the yield of the total liquid products (ΣC$_{7+}$) determined from flash Py-GC analysis as FPΣC$_{7+}$. This has a very poor correlation with Rock-Eval QI but a much better correlation with MCPΣC$_{8+}$ for the 17 coals with R^2 = 0.30 and 0.70, respectively (Fig. 7a and b). FPΣC$_{7+}$ appears to be a better indicator of oil potential than Rock-Eval QI for coal samples. Coals from the Junggar Basin have higher FPΣC$_{7+}$ and MCPΣC$_{8+}$ than those from the Kuqa Depression having similar QI, indicating that the former have higher oil potentials than the latter (Table 1, Figs. 6a and 7a). These results can be ascribed to the following causes: (1) FPΣC$_{7+}$ values do not include the yields of smaller released components (FPΣC$_{1-6}$) while Rock-Eval QI values are the yields of all released components, partly leading to the result that Rock-Eval QI values are substantially higher than FPΣC$_{7+}$ values (Table 1, Figs. 6a and 7a). However, QI/FPΣC$_{7+}$ ratios range from 1.39 to 3.87. For example, QI and FPΣC$_{7+}$ are 173 and 124 mg/g TOC, respectively for Junggar coal JC23 but they are 265 and 68 mg/g TOC, respectively for Kuqa coal TTC18 (Table 1, Fig. 7a). FPΣC$_{1-6}$ yields cannot account for the total difference between Rock-Eval QI and FPΣC$_{7+}$ from flash Py-GC; (2) residual coal kerogen retains a higher portion of bound moieties after flash Py-GC analysis due to the short heating duration (650 °C for 20 s), compared with that after Rock-Eval analysis. Coals with higher oil potentials (MCPΣC$_{8+}$) can release a higher portion of bound moieties than those with lower oil potentials and similar QI in flash Py-GC; (3) The released products from coals can be fully detected by FID in Rock-Eval analysis. In contrast, a substantial portion of the released products are retained in the injector and column of gas chromatography in flash Py-GC. Coals with higher oil potentials (CPΣC$_{8+}$) generate a higher portion of components eluting through the injector and column and thus are detected by FID in flash Py-GC than those with lower oil potentials and similar QI; (4) In flash Py-GC analysis, the released components which elute through the injector and column and are
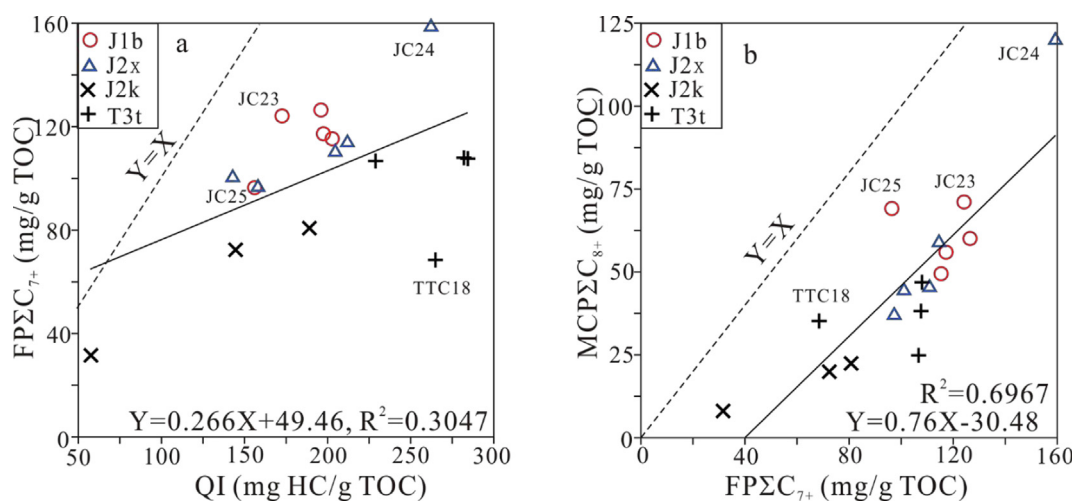

Fig. 7. Crossplots of Rock-Eval QI vs FPΣC$_{7+}$ from flash Py-GC (a) and FPΣC$_{7+}$ from flash Py-GC vs the maximum CPΣC$_{8+}$ from confined pyrolysis (b).

detected by FID have lower aromaticity or/and lower polarity compared with those which are retained in the injector and column and the bound moieties in the residual coal kerogen. The former can generate higher amount of oil compared with the latter in confined pyrolysis and geological condition. Therefore, $FP\Sigma C_{7+}$ values have better correlations with $MCP\Sigma C_{8+}$ than Rock-Eval QI.

It is noteworthy that coals JC23, JC24 and JC25 collected from the Sikeshu Sag in the southwestern Junggar Basin, have the highest $MCP\Sigma C_{8+}$ values and $MCP\Sigma C_{8+}/QI$ ratios even though they have relatively lower QI values among the 17 coals in the present study (Table 1, Figs. 6 and 7), possibly demonstrating that coal beds in the Sikeshu Sag in the Junggar Basin have higher oil generative potentials. To date, most oilfields which were derived from the Jurassic coaly source rocks are found within and around this sag in the Junggar Basin (Fig. 1).

4.4. Predicting gas to oil ratio (GOR)

GOR is a critical factor controlling petroleum phase behavior and physical properties (Di Primio and Horsfield, 2006). It is very useful to find an approach to predict GOR of petroleum generated from coals on the basis of geochemical parameters from Rock-Eval and Py-GC analyses. We defined the yield of gaseous hydrocarbons (ΣC_{1-5}) in confined pyrolysis as $CP\Sigma C_{1-5}$. For the 17 coals, $CP\Sigma C_{1-5}$ values increase with temperature and maturity (Fig. 8). $CP\Sigma C_{1-5}$ values and the ratios of $CP\Sigma C_{1-5}$ to $CP\Sigma C_{8+}$ ($CP\Sigma C_{1-5}/\Sigma C_{8+}$) at the maturity for $MCP\Sigma C_{8+}$ of the 17 coals are shown in Table 1. di Primio and Horsfield (2006) suggested that the mass proportions of the total gaseous hydrocarbons and liquid components generated from kerogen pyrolysis in closed system are comparable to natural petroleum. The $CP\Sigma C_{1-5}/\Sigma C_{8+}$ ratio at the maturity for $MCP\Sigma C_{8+}$ reflects gas to oil ratio (GOR) for petroleum fluids generated from a coal in confined pyrolysis, as well as in geological situations.

$CP\Sigma C_{1-5}/\Sigma C_{8+}$ ratio has no clear correlation with Rock-Eval QI for these 17 coals (Fig. 9a). However, the $CP\Sigma C_{1-5}/\Sigma C_{8+}$ ratio has a clear negative correlation with $MCP\Sigma C_{8+}$, demonstrating that this ratio decreases with oil potential for these coals (Fig. 9b). The $CP\Sigma C_{1-5}/\Sigma C_{8+}$ ratio has a better negative correlation with $FP\Sigma n$-C_{7+} and best negative correlation with $FP\Sigma n$-$C_{7+}/\Sigma C_{7+}$ ratio obtained from flash Py-GC (Fig. 9c and d), demonstrating that the $CP\Sigma C_{1-5}/\Sigma C_{8+}$ ratio is controlled by the concentration of bound n-alkanes and, in particular, the relative concentration of bound n-alkanes to the total bound moieties in the kerogen of humic coals. Coal JC30 has the highest $FP\Sigma n$-$C_{7+}/\Sigma C_{7+}$ ratio, and therefore the lowest $CP\Sigma C_{1-5}/\Sigma C_{8+}$ ratio among the 17 coals (Table 1, Fig. 9b–d), although coal JC24 has higher $MCP\Sigma C_{8+}$ and $FP\Sigma n$-C_{7+} values than coal JC30 (Table 1, Fig. 9b and c).

Coals JC23, JC24 and JC25 from the Sikeshu Sag of the southwestern Junggar Basin (Fig. 1b) have $CP\Sigma C_{1-5}/\Sigma C_{8+}$ ratios in the range of 0.44–0.51 mg/mg from confined pyrolysis (Table 1). On the basis of correlation between $CP\Sigma C_{1-5}/\Sigma C_{8+}$ and $FP\Sigma n$-$C_{7+}/\Sigma C_{7+}$ ratios (Fig. 9d): $CP\Sigma C_{1-5}/\Sigma C_{8+} = -1.64 \times (FP\Sigma n$-$C_{7+}/\Sigma C_{7+})$ + 0.95, the predicted $CP\Sigma C_{1-5}/\Sigma C_{8+}$ ratios for these three coals are in the range of 0.45–0.48 mg/mg. $CP\Sigma C_{8+}$ values are not equal to oil yields generated from kerogen or coal samples as demonstrated in previous studies (Xiang et al., 2016; Huang et al., 2019). Therefore, $CP\Sigma C_{1-5}/\Sigma C_{8+}$ ratios are not equal to gas/oil ratios in confined pyrolysis for these coals. Eighteen non-biodegraded light oils from the Junggar Basin have yields of liquid components (ΣC_{8+}) in the range of 425–715 mg/g oil with an average of 563 mg/g oil, measured from gas chromatograms on the basis of two internal standards of deuterated n-C_{22} and n-C_{24} n-alkanes, the same method to determine the yield of liquid components ($CP\Sigma C_{8+}$) in confined pyrolysis (Huang et al., 2019). Therefore, GOR values should be calculated using the formula: GOR = 0.563 $\times$ ($CP\Sigma C_{1-5}/\Sigma C_{8+}$). GOR
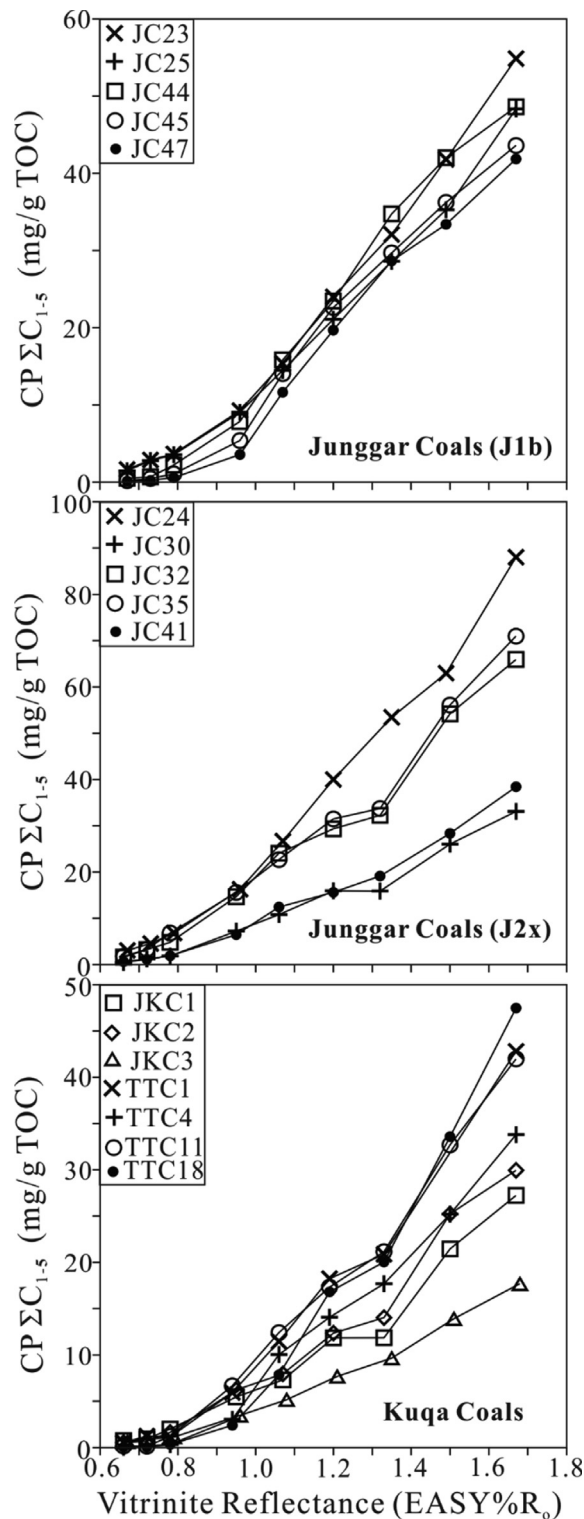

Fig. 8. Yields of total gas components ($CP\Sigma C_{1-5}$) in confined pyrolysis for the 17 coals from 322 °C to 431 °C at a heating rate 2 °C/h (EASY%Ro 0.66–1.67) in confined pyrolysis experiments (data for the seven coals from Kuqa Depression from Huang et al., 2019).

ratios of coals JC23, JC24 and JC25 are in the range of 0.25–0.29 from confined pyrolysis, and 0.25–0.27 predicted based on the $FP\Sigma n$-$C_{7+}/\Sigma C_{7+}$ ratio from flash Py-GC analysis (Fig. 9d). This result is consistent with the GOR ratio for the Gaoquan oilfield near the locations of these three coals (Fig. 1a), on the basis of oil test result
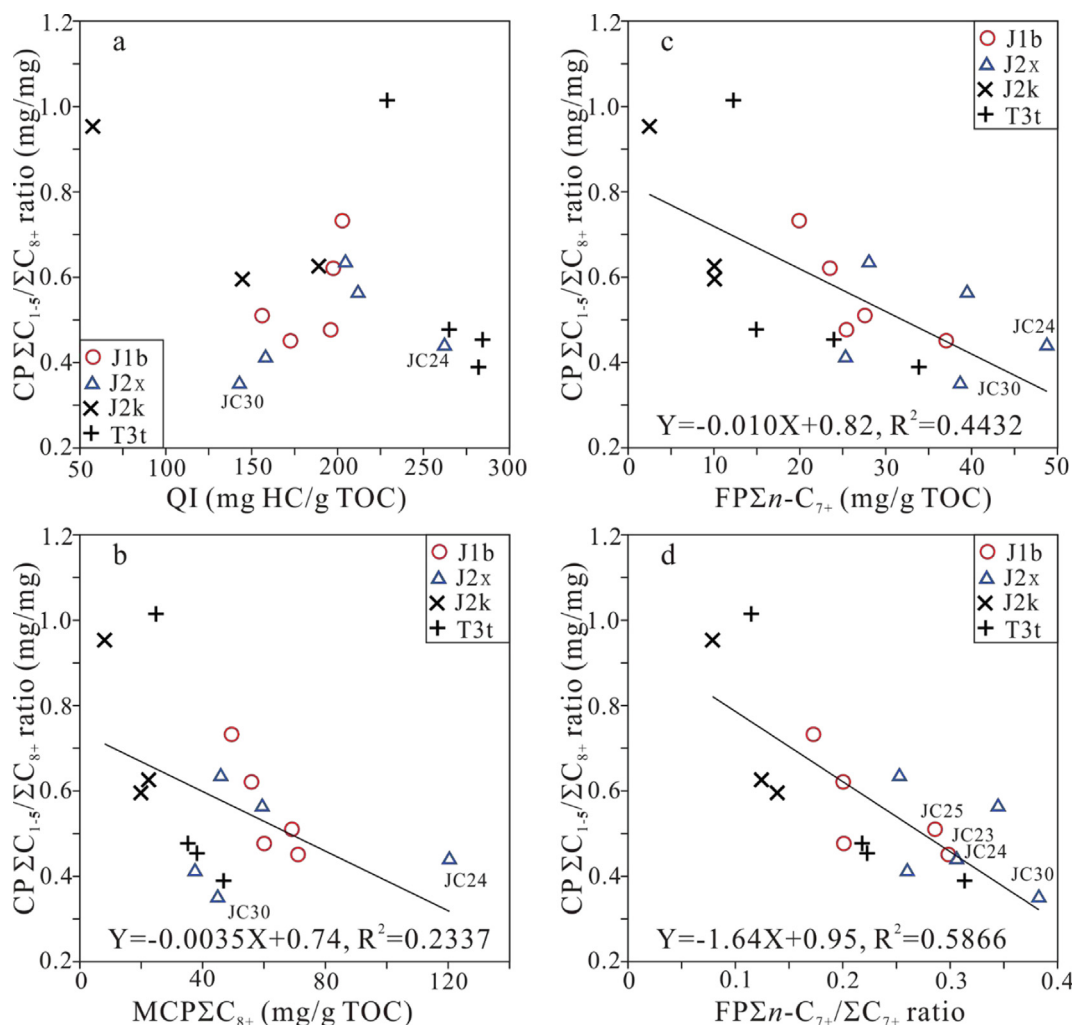
Fig. 9. Crossplots of $CP\Sigma C_{1-5}/\Sigma C_{8+}$ ratio from confined pyrolysis vs Rock-Eval QI (a), the maximum $CP\Sigma C_{8+}$ from confined pyrolysis (b), $FP\Sigma n\text{-}C_{7+}$ from flash Py-GC (c) and $FP\Sigma n\text{-}C_{7+}/\Sigma C_{7+}$ ratio from flash Py-GC (d).

for borehole GT1, i.e., 1213 m^3 of oil and 322 × 10^3 m^3 of gas per day (Du et al., 2019), equivalent to a GOR of 0.262 mg/mg with oil and gas densities of 0.824 g/ml and 0.813 × 10^{-3} g/ml, respectively (Du et al., 2019).

4.5. H/C atomic ratio

The H/C atomic ratio is a widely used parameter to indicate chemical composition and hydrocarbon generative capabilities of coal and kerogen samples (e.g., Van Krevelen, 1961; Tissot and Welte, 1984). Correlation is better between the H/C ratio and $MCP\Sigma C_{8+}$ than between Rock-Eval QI and $MCP\Sigma C_{8+}$ (Figs. 6a and 10a). However, the correlation is much poorer between the H/C ratio and $MCP\Sigma C_{8+}$ than that between $FP\Sigma n\text{-}C_{7+}$ and $MCP\Sigma C_{8+}$ (Figs. 6c and 10a), and even poorer than that between $FP\Sigma C_{7+}$ and $MCP\Sigma C_{8+}$ (Figs. 7b and 10a).

The H/C ratio has a better negative correlation with $CP\Sigma C_{1-5}/\Sigma C_{8+}$ (GOR indicator) than QI with $CP\Sigma C_{1-5}/\Sigma C_{8+}$ (Figs. 9a and 10b). However, the correlation of the H/C ratio with $CP\Sigma C_{1-5}/\Sigma C_{8+}$ is much poorer than those of $MCP\Sigma C_{8+}$, $FP\Sigma n\text{-}C_{7+}$ and the ratio of $FP\Sigma n\text{-}C_{7+}/FP\Sigma C_{7+}$ with $CP\Sigma C_{1-5}/\Sigma C_{8+}$ (Figs. 9b–d, 10b). Furthermore, it is noteworthy that the H/C ratio has almost no correlation with QI for the analyzed coals (Fig. 10c).

4.6. Criteria for coals as potential oil source rocks

Hunt (1991) suggested that the coals with H/C >~0.9, or HI >~200 mg HC/g TOC and liptinite contents >15% have the potential to generate and release oil as well as gas. Among the 17 coals in the present study, eight coals, i.e., four coals from the Junggar Basin (JC45, JC24, JC32 and JC35) and four coals from the Kuqa Depression (TTC1, TTC4, TTC11 and TTC18), have QI > 200 mg HC/g TOC while the other nine coals have QI < 200 mg HC/g TOC (Table 1). Only three coals JC24, JC32 and JC35 from the Junggar Basin have an H/C atomic ratio > 0.9 while the other 14 coals have this ratio < 0.90 (Table 1). Killops et al. (1998) suggested a threshold oil amount of 40 mg/g TOC is needed for oil expulsion from coal. As mentioned earlier, 1 mg oil is equivalent to about 0.563 mg liquid components (ΣC_{8+}). Coals with yield of $MCP\Sigma C_{8+}$ >~22.5 mg/g TOC can be effective oil source rocks. On the basis of correlation between $MCP\Sigma C_{8+}$ yield in confined pyrolysis and $FP\Sigma n\text{-}C_{7+}$ yield from flash Py-GC: $MCP\Sigma C_{8+}$ = 1.75 × $FP\Sigma n\text{-}C_{7+}$ + 4.28 with R^2 = 0.71 (Fig. 6c), coals with $FP\Sigma n\text{-}C_{7+}$ yield > 10.4 mg/g TOC from flash Py-GC analysis can generate $MCP\Sigma C_{8+}$ yield >~22.5 mg/g TOC or oil yield >~40 mg/g TOC in confined pyrolysis or natural system. For the 17 coals studied, only three coals JKC1, JKC2 and JKC3 from the Kuqa Depression have $FP\Sigma n\text{-}C_{7+}$ yield < 10.4 mg/g TOC and are ineffective oil source rocks while all the other 14 coals have

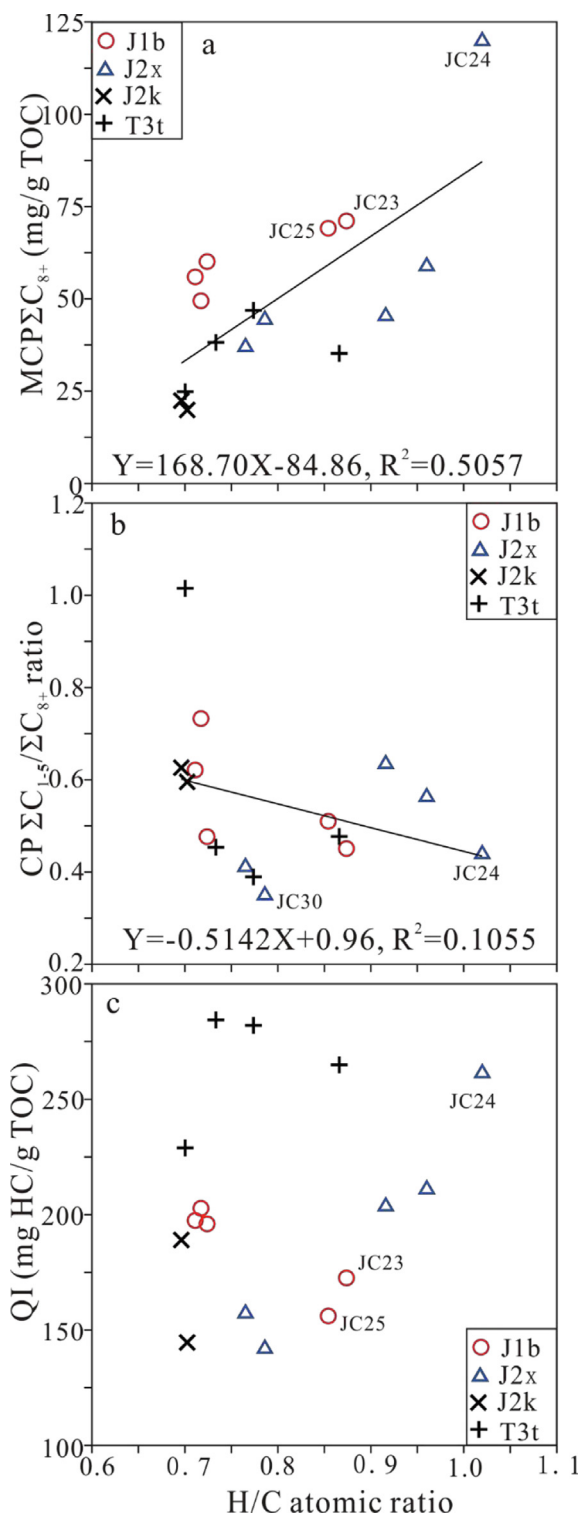**Fig. 10.** Crossplots of H/C atomic ratio vs the maximum $CP\Sigma C_{8+}$ from confined pyrolysis (a), $CP\Sigma C_{1-5}/\Sigma C_{8+}$ ratio from confined pyrolysis (b) and Rock-Eval QI (c).

$FP\Sigma n\text{-}C_{7+}$ yield > 10.4 mg/g TOC and are effective oil source rocks (Table 1).

5. Conclusions

For the 17 coals studied here, $MCP\Sigma C_{8+}$ values from confined pyrolysis, which reflect the oil potential, have close correlations

with concentrations of bound n-alkanes ($FP\Sigma n\text{-}C_{7+}$) released in flash Py-GC, but have poor correlations with Rock-Eval QI values. Thus, the oil potential of coals can be better predicted on the basis of $FP\Sigma n\text{-}C_{7+}$ yields from flash Py-GC analysis. Coals with a $FP\Sigma n\text{-}C_{7+}$ yield >10.4 mg/g TOC can generate $MCP\Sigma C_{8+}$ yield >$\sim$22.5 mg/g TOC or oil yield >$\sim$40 mg/g TOC in confined pyrolysis or natural system and are effective oil source rocks.

The correlations of parameters with gas to oil ratios (GOR) within the oil generative window in confined pyrolysis experiments are increasingly better in the sequence of Rock-Eval QI, H/C atomic ratio, maximum $CP\Sigma C_{8+}$, $FP\Sigma n\text{-}C_{7+}$ and $FP\Sigma n\text{-}C_{7+}/\Sigma C_{7+}$ ratio. The GOR of petroleum generated from coals can be reasonably predicted on the basis of the $FP\Sigma n\text{-}C_{7+}/\Sigma C_{7+}$ ratio from flash Py-GC analysis.

Declaration of Competing Interest

The authors declare that they have no known competing financial interests or personal relationships that could have appeared to influence the work reported in this paper.

Appendix A. Supplementary material

Supplementary data to this article can be found online at https://doi.org/10.1016/j.orggeochem.2020.104097.

*Associate Editor—***Dariusz Strąpoć**

References

Boreham, C.J., Horsfield, B., Schenk, H.J., 1999. Predicting the quantities of oil and gas generated from Australian Permian coals, Bowen Basin using pyrolytic methods. Marine and Petroleum Geology 16, 165–188.

Burnham, A.K., Braun, R.L., 2017. Simple relative sorptivity model of petroleum expulsion. Energy & Fuels 31, 9308–9318.

Chen, J., Liang, D., Wang, X., Zhong, N., Song, F., Deng, C., Shi, X., Jin, T., Xiang, S., 2003a. Mixed oils derived from multiple source rocks in the Cainan oilfield, Junggar Basin, Northwest China. Part I: genetic potential of source rocks, features of biomarkers and oil sources of typical crude oils. Organic Geochemistry 34, 889–909.

Chen, J., Deng, C., Liang, D., Wang, X., Zhong, N., Song, F., Shi, X., Jin, T., Xiang, S., 2003b. Mixed oils derived from multiple source rocks in the Cainan oilfield, Junggar Basin, Northwest China. Part II: artificial mixing experiments on typical crude oils and quantitative oil-source correlation. Organic Geochemistry 34, 911–930.

Chen, J., Wang, X., Deng, C., Zhao, Z., Ni, Y., Sun, Y., Yang, H., Wang, H., Liang, D., 2015. Geochemical features and classification of crude oil in the southern margin of Junggar Basin, Northwestern China. Acta Petrolei Sinica 36, 1315–1331 (in Chinese).

Curry, D.J., 1995. The pyrolysis yield index: a rapid and reproducible technique for estimating the oil generation potential of coals and terrigenous kerogens. In: Grimalt, J.O., Dorronsoro, C. (Eds.), Organic Geochemistry: Developments and Applications to Energy, Climate, Environment and Human History, Selected papers from the 17th International Meeting on Organic Geochemistry, pp. 763–766.

Curry, D.J., Bohacs, K.M., Diessel, C.F.K., Gammidge, L.C., Rigby, R., 1995. Sequence stratigraphic and depositional environment controls on the geochemistry and oil generation potential of coals and terrigenous kerogens. In: Grimalt, J.O., Dorronsoro, C. (Eds.), Organic Geochemistry: Developments and Applications to Energy, Climate, Environment and Human History, Selected papers from the 17th International Meeting on Organic Geochemistry, pp. 138–141.

Curry, D.J., Emmett, J.K., Hunt, J.W., 1994. Geochemistry of aliphatic-rich coals in the Cooper Basin, Australia and Taranaki basin, New Zealand: implications for the occurrence of potentially oil-generative coals. In: Scott, A.C., Fleet, A.J. (Eds.), Coal and Coal-bearing Strata as Oil-prone Source Rocks? Geological Society Special Publication No. 77, pp. 149–182.

Derenne, S., Largeau, C., Casadevall, E., Sinninghe Damsté, J.S., Tegelaar, E.W., de Leeuw, J.W., 1990. Characterization of Estonian kukersite by spectroscopy and pyrolysis: evidence for abundant alkyl phenolic moieties in an Ordovician, marine, type II/I kerogen. Organic Geochemistry 16, 873–888.

Dieckmann, V., Ondrak, R., Cramer, B., Horsfield, B., 2006. Deep basin gas: new insights from kinetic modeling and isotopic fractionation in deep-formed gas precursors. Marine and Petroleum Geology 23, 183–199.

di Primio, R., Horsfield, B., 2006. From petroleum-type organofacies to hydrocarbon phase prediction. American Association of Petroleum Geologists Bulletin 90, 1031–1058.

Du, J., Zhi, D., Li, J., Yang, D., Tang, Y., Qi, X., Xiao, L., Wei, L., 2019. Major breakthrough of well Gaotan 1 and exploration prospects of lower assemblage in southern margin of Junggar Basin, NW China. Petroleum Exploration and Development 46, 205–215 (in Chinese).

Erdmann, M., Horsfield, B., 2006. Enhanced late gas generation potential of petroleum source rocks via recombination reactions: evidence from the Norwegian North Sea. Geochimica et Cosmochimica Acta 70, 3943–3956.

Eglinton, T.I., Philp, R.P., Rowland, S.J., 1988. Flash pyrolysis of artificially matured kerogens from the Kimmeridge Clay, U.K. Organic Geochemistry 12, 33–41.

Eglinton, T.I., Larter, S.R., Boon, J.J., 1991. Characterisation of kerogens, coals and asphaltenes by quantitative pyrolysis-mass spectrometry. Journal of Analytical and Applied Pyrolysis 20, 25–45.

Hill, R.J., Tang, Y., Kaplan, I.R., 2003. Insight into oil cracking based on laboratory experiments. Organic Geochemistry 34, 1651–1672.

Horsfield, B., 1989. Practical criteria for classifying kerogens: some observations from pyrolysis-gas chromatography. Geochimica et Cosmochimica Acta 53, 891–901.

Huang, W., Zeng, L., Pan, C., Xiao, Z., Zhang, H., Huang, Z., Zhao, Q., Yu, S., Xu, H., Chen, C., Liu, D., Liu, J., 2019. Petroleum generation potentials and kinetics of coaly source rocks in the Kuqa Depression of Tarim Basin, northwest China. Organic Geochemistry 133, 32–52.

Hunt, J.M., 1991. Generation of gas and oil from coal and other terrestrial organic matter. Organic Geochemistry 17, 673–680.

Isaksen, G.H., Curry, D.J., Yeakel, J.D., Jenssen, A.I., 1998. Controls on the oil and gas potential of humic coals. Organic Geochemistry 29, 22–44.

Katz, B.J., Kelley, P.A., Royle, R.A., Jorjorian, T., 1991. Hydrocarbon products of coals as revealed by pyrolysis-gas chromatography. Organic Geochemistry 17, 711–722.

Killops, S.D., Funnell, R.H., Suggate, R.P., Sykes, R., Peters, K.E., Walters, C.C., Woolhouse, A.D., Weston, R.J., Boudou, J.P., 1998. Predicting generation and expulsion of paraffinic oil from vitrinite-rich coals. Organic Geochemistry 29, 1–21.

Largeau, C., 1984. Formation of *Botryococcus*-derived kerogens. Comparative study of immature Torbanite and of the extant alga *Botryococcus braunii*. Organic Geochemistry 8, 327–332.

Larter, S.R., Douglas, A.G., 1980. A pyrolysis-gas chromatographic method for kerogen typing. In: Douglas, A.G., Maxwell, G.R. (Eds.), Advances in Organic Geochemistry. Pergamon, Oxford, pp. 579–584.

Li, E., Pan, C., Yu, S., Jin, X., Liu, J., 2013. Hydrocarbon generation from coal, extracted coal and bitumen rich coal in confined pyrolysis experiments. Organic Geochemistry 64, 58–75.

Li, E., Pan, C., Yu, S., Jin, X., Liu, J., 2016. Interaction of coal and oil in confined pyrolysis experiments: insight from the yields and carbon isotopes of gas and liquid hydrocarbons. Marine and Petroleum Geology 69, 13–37.

Liang, D., Zhang, S., Chen, J., Wang, F., Wang, P., 2003. Organic geochemistry of oil and gas in the Kuqa depression, Tarim Basin, NW China. Organic Geochemistry 34, 873–888.

Liao, Y., Zheng, Y., Pan, Y., Sun, Y., Geng, A., 2015. A method to quantify C_1–C_5 hydrocarbon gases by kerogen primary cracking using pyrolysis gas chromatography. Organic Geochemistry 79, 49–55.

Mansuy, L., Landais, P., Ruau, O., 1995. Importance of the reacting medium in artificial maturation of a coal by confined pyrolysis. 1. Hydrocarbons and polar compounds. Energy & Fuels 9, 691–703.

Mansuy, L., Landais, P., 1995. Importance of the reacting medium in artificial maturation of a coal by confined pyrolysis. 2. Water and polar compounds. Energy & Fuels, 809–821.

McNeil, R.I., BeMent, W.O., 1996. Thermal stability of hydrocarbons: laboratory criteria. Energy & Fuels 10, 60–67.

Michels, R., Burkle, V., Mansuy, L., Langlois, E., Ruau, O., Landais, P., 2000. Role of polar compounds as source of hydrocarbons and reactive medium during the artificial maturation of Mahakam coal. Energy & Fuels 14, 1059–1071.

Monthioux, M., Landais, P., Monin, J.C., 1985. Comparison between natural and artificial maturation series of humic coals from the Mahakam Delta, Indonesia. Organic Geochemistry 8, 275–292.

Monthioux, M., Landais, P., Durand, B., 1986. Comparison between extracts from natural and artificial maturation series of Mahakam Delta coals. Organic Geochemistry 10, 299–311.

Pan, C., Jiang, L., Liu, J., Zhang, S., Zhu, G., 2012. The effects of pyrobitumen on oil cracking in confined pyrolysis experiments. Organic Geochemistry 45, 29–47.

Pan, Y., Liao, Y., Zheng, Y., 2015. Effect of biodegradation on the molecular composition and structure of asphaltenes: clues from quantitative Py-GC and THM-GC. Organic Geochemistry 86, 32–44.

Pepper, A.S., Corvi, P.J., 1995. Simple kinetic models of petroleum formation. Part I: oil and gas generation from kerogen. Marine and Petroleum Geology 12, 291–319.

Peters, K.E., 1986. Guidelines for evaluating petroleum source rock using programmed pyrolysis. American Association of Petroleum Geologists Bulletin 70, 318–329.

Peters, K.E., Walters, C.C., Moldowan, J.M., 2005. The Biomarker Guide. Biomarkers and Isotopes in Petroleum Exploration and Earth History, vol. 1. Cambridge University Press, UK, pp. 1155.

Powell, T.G., Boreham, C.J., 1991. Petroleum generation and source rock assessment in terrigenous sequences: an update. Australian Petroleum Exploration Association Journal 31, 297–311.

Price, L.C., Wenger, L.M., 1992. The influence of pressure on petroleum generation and maturation as suggested by aqueous pyrolysis. Organic Geochemistry 19, 141–159.

Sykes, R., Snowdon, L.R., 2002. Guidelines for assessing the petroleum potential of coaly source rocks using Rock-Eval pyrolysis. Organic Geochemistry 33, 1441–1455.

Sun, P., Bian, B., Yuan, Y., Zhang, X., Cao, J., 2015. Natural gas in southern Junggar Basin in northwest China: geochemistry and origin. Geochimica 44, 275–288 (in Chinese).

Sweeney, J.J., Burnham, A.K., 1990. Evaluation of a simple model of vitrinite reflectance based on chemical kinetics. American Association of Petroleum Geologists Bulletin 74, 1559–1570.

Tegelaar, E.W., Noble, R.A., 1994. Kinetics of hydrocarbon generation as a function of the molecular structure of kerogen as revealed by pyrolysis–gas chromatography. Organic Geochemistry 22, 543–574.

Tissot, B.P., Welte, D.H., 1984. Petroleum Formation and Occurrence. Springer-Verlag, Berlin.

Van Krevelen, D.W., 1961. Coal. Elsevier, Amsterdam.

Wang, X., Zhi, D., Wang, Y., Chen, J., Qin, Z., Liu, D., Xiang, Y., Lan, W., Li, N., 2013. Source Rocks and Oil-Gas Geochemistry in Junggar Basin. Chinese Petroleum Industry Press, 565 pp. (in Chinese).

Wang, Z., 2014. Formation mechanism and enrichment regularities of Kelasu subsalt deep large gas field in Kuqa Depression, Tarim Basin. Natural Gas Geoscience 25, 153–166 (in Chinese).

Xiang, B., Li, E., Gao, X., Wang, M., Wang, Y., Xu, H., Huang, P., Yu, S., Liu, J., Zou, Y., Pan, C., 2016. Petroleum generation kinetics for Permian lacustrine source rocks in the Junggar Basin, NW China. Organic Geochemistry 77, 1–17.

Xiao, F., Liu, L., Zhang, Z., Wu, K., Xu, Z., Zhou, C., 2014. Conflicting sterane and aromatic maturity parameters in Neogene light oils, eastern Chepaizi High, Junggar Basin, NW China. Organic Geochemistry 76, 48–61.

Zhao, W., Zhang, S., Wang, F., Cramer, B., Chen, J., Sun, Y., Zhang, B., Zhao, M., 2005. Gas systems in the Kuche Depression of the Tarim Basin: source rock distributions, generation kinetics and gas accumulation history. Organic Geochemistry 36, 1583–1601.